



**HAL**  
open science

## Water cast film formability of sugarcane bagasse xylans favored by side groups

Zhouyang Xiang, Xuchen Jin, Caoxing Huang, Lian Li, Wanhua Wu, Haisong Qi, Yoshiharu Nishiyama

### ► To cite this version:

Zhouyang Xiang, Xuchen Jin, Caoxing Huang, Lian Li, Wanhua Wu, et al.. Water cast film formability of sugarcane bagasse xylans favored by side groups. *Cellulose*, 2020, 27 (13), pp.7307-7320. 10.1007/s10570-020-03291-7 . hal-02951278

**HAL Id: hal-02951278**

**<https://hal.science/hal-02951278>**

Submitted on 13 Nov 2020

**HAL** is a multi-disciplinary open access archive for the deposit and dissemination of scientific research documents, whether they are published or not. The documents may come from teaching and research institutions in France or abroad, or from public or private research centers.

L'archive ouverte pluridisciplinaire **HAL**, est destinée au dépôt et à la diffusion de documents scientifiques de niveau recherche, publiés ou non, émanant des établissements d'enseignement et de recherche français ou étrangers, des laboratoires publics ou privés.

1 **Water Cast Film Formability of Sugarcane Bagasse Xylans Favored**  
2 **by Side Groups**

3 **Zhouyang Xiang,<sup>1,\*</sup> Xuchen Jin,<sup>1</sup> Caoxing Huang,<sup>2</sup> Lian Li,<sup>1</sup> Wanhua Wu,<sup>1</sup> Haisong Qi,<sup>1</sup>**  
4 **Yoshiharu Nishiyama<sup>3</sup>**

5 *<sup>1</sup>State Key Laboratory of Pulp and Paper Engineering, South China University of Technology,*  
6 *Guangzhou 510640, China*

7 *<sup>2</sup>Jiangsu Co-Innovation Center of Efficient Processing and Utilization of Forest Resources,*  
8 *Nanjing Forestry University, Nanjing 210037, China*

9 *<sup>3</sup>University Grenoble Alpes, CNRS, CERMAV, Grenoble 38058, France*

10 \*Corresponding authors: Email: fezyxiang@scut.edu.cn; Tel: +86-20-87113753  
11

12 **ABSTRACT:** Hemicellulose, one of the most abundant biopolymers next to cellulose, has been  
13 considered as a potential substitute to synthetic polymers. Film casting from water is the most  
14 basic route for material applications of xylan. However, depending on plant sources and  
15 separation methods, xylans do not always form films and the related mechanism is unclear,  
16 which significantly hinders their material applications. We extensively characterized various  
17 fractions of bagasse xylan to understand the molecular features promoting the film formation.  
18 The side groups of xylans or impurities contributed to the prevention of excessive aggregation or  
19 crystallization of xylan molecules, leading to the film-forming capacity. However, once the film  
20 is formed, the side groups do not seem to be necessarily contributing to the mechanical  
21 resistance.

22 **Keywords:** Xylan; Crystallization; Side group; Film formation; Mechanical property

## 23 **Introduction**

24 Polysaccharides in plant secondary cell walls are the most abundant renewable biopolymers  
25 on Earth, among which hemicelluloses are the second most abundant after cellulose (Huang et al.,  
26 2019a; Lin et al., 2019). Hemicelluloses are a group of hetero-polysaccharides with highly  
27 diversified structures incorporating various sugars. Hemicelluloses extracted from hardwood and  
28 graminaceous plants are primarily xylans, which is relatively easy to be separated and processed  
29 compared to other types of hemicellulose such as glucomannans from softwood. Generally,  
30 xylans have  $\beta$ -(1-4)-linked D-xylopyranosyl backbone but are heavily substituted in native state  
31 with substituents mainly including  $\alpha$ -L-arabinofuranosyl,  $\alpha$ -D-glucuronopyranosyl units or/and  
32 4-*O*-methyl- $\alpha$ -D-glucuronopyranosyl units; most xylans are partially acetylated (Ebringerova  
33 and Heinze, 2000; Morais de Carvalho et al., 2017; Spiridon and Popa, 2008; Sun et al., 2000).  
34 From different plant sources, the chemical structure of xylans also varies. In hardwood, xylans  
35 do not have arabinofuranosyl substitutions, which are specifically termed as glucuronoxylans.  
36 The xylans from woody tissues of grasses and annual plants are specifically termed as  
37 glucuronoarabinoxylans; they have 2-linked (4-*O*-methyl)-glucuronopyranosyl units and  
38 3-linked arabinofuranosyl units on the xylopyranosyl backbone. The xylans from cereal grains  
39 are usually termed as arabinoxylans, in which, the backbone xylopyranosyl units can be mono-  
40 or di-substituted at positions 2 or/and 3 by the arabinofuranosyl units (Ebringerova and Heinze,  
41 2000; Morais de Carvalho et al., 2017; Spiridon and Popa, 2008).

42 As a naturally abundant and water dispersible biopolymer, xylan has been considered as a  
43 potential substitute to the petroleum-based synthetic polymers (Hansen and Plackett, 2008).  
44 However, xylan films generally have inferior mechanical properties, which usually leads to  
45 excessive chemical modifications with high cost and high environmental impact which leads to

46 no advantage over the petroleum-based synthetic polymers. The major hurdle in the application  
47 of originally separated xylans is their highly diversified chemical structures and our inadequate  
48 understanding of the mechanism between mechanical properties and their structures.

49 Film casting from water is the most basic route for material applications of xylan. However,  
50 depending on plant sources and separation methods, xylan does not always form films. For  
51 example, xylan from barley husk (Hoije et al., 2005) and distillers' grains (Xiang et al., 2014)  
52 always forms films, while xylan from hardwood requires the addition of plasticizer to form films  
53 (Grondahl et al., 2004); from our previous study and as revisited in this study, xylan extracted  
54 from sugarcane bagasse with 2% NaOH forms films very well, while xylan extracted with 4% or  
55 6% NaOH does not form films even with the addition of a plasticizer (Jin et al., 2019). The  
56 unpredictable film formability of xylan greatly hinders its rational separation strategy for  
57 material applications. Works on enzymatically or chemically tailored xylan suggested that the  
58 presence of lignin promotes (Goksu et al., 2007), while the degree of substitution does not affect  
59 the film formability of xylan (Hoije et al., 2008; Sternemalm et al., 2008). However, many  
60 structural aspects still await investigation and a key question, examined here, is the relation  
61 between xylan molecular architecture and its film formability.

62 The side groups of xylan are known to prevent the intermolecular aggregation, which  
63 happens for a linear molecule such as cellulose that tends to crystallize. The side groups would  
64 thus greatly affect the properties of xylan (Dea et al., 1973; Hoije et al., 2008; Shrestha et al.,  
65 2019). The solubility of xylan in water decreased with decreasing number of side groups as the  
66 unsubstituted segments would aggregate into insoluble form (Andrewartha et al., 1979). The side  
67 groups of xylan can also be responsible for the high viscosity of xylan solution by restricting the  
68 mobility of xylan backbone (Andrewartha et al., 1979; Sternemalm et al., 2008).

69 Xylan is generally known as an amorphous polymer. However, with reduced number of side  
70 groups, xylan can form hydrous and anhydrous crystals (Dea et al., 1973; Hoije et al., 2008;  
71 Horio and Imamura, 1964; Kobayashi et al., 2013; Marchessault and Timell, 1960; Nieduszynski  
72 and Marchessault, 1972), which greatly hinders the polymer internal rotation and thus increase  
73 the rigidity (Arinstein et al., 2007; De Rosa et al., 2006; Fama et al., 2005; Shrestha et al., 2019).  
74 A moderate degree of branching or an addition of external plasticizers may ensure flexibility of  
75 xylan films by increasing free volume (Grondahl et al., 2004; Hansen and Plackett, 2008; Hoije  
76 et al., 2008). However, some studies also found that external plasticizer may promote the  
77 crystallinity of xylan films due to the increased chain mobility (Mikkonen et al., 2009). Our  
78 previous studies showed that xylans with higher molecular weight and smaller number of side  
79 groups produced films with higher tensile strength and modulus of elasticity; lignin can act either  
80 as an impurity (detrimental to the film strength) or as a reinforcement to the films depending on  
81 the molecular weights of xylan (Jin et al., 2019).

82 The addition of external plasticizers or biopolymers, e.g. sorbitol, xylitol, chitosan, gluten,  
83 often helps the film formation of xylan (Gabrielii and Gatenholm, 1998; Grondahl et al., 2004;  
84 Kayserilioglu et al., 2003). However, xylans with the same molecular weight and lignin content  
85 may or may not form a film and the underlying mechanism for film formability is unclear. In this  
86 study, we chose alkali-extraction as one of the scalable extraction techniques that can be easily  
87 implemented in the laboratory, though it inevitably removes the acetyl groups. We prepared  
88 various xylan fractions by modulating extraction and precipitation methods, i.e. alkali extraction  
89 method, sequential alkali extraction method, graded ethanol precipitation, I<sub>2</sub>-KI precipitation and  
90 ammonium sulfate precipitation methods. We studied the chemical structures, solution properties,  
91 particle morphology, and film microstructures to relate with the film formability of xylans.

92 **Materials and Methods**

93 *Separation of xylan*

94 Grounded sugarcane bagasse sample sieved between 40 and 60 mesh was extracted in a  
 95 Soxhlet extractor with 95% ethanol for 6 hours to remove extractives, fat and wax. The dewaxed  
 96 bagasse was dried in an oven at 60 °C until moisture content reduced to ~4%. The types of  
 97 separation methods of xylan used in this study are summarized in Tables 1.

98 Approximately 20 g dewaxed bagasse was extracted in 240 ml of 2%, 4% or 6% NaOH  
 99 solution or sequentially by 2 and 4% or 2, 4 and 6% NaOH solutions. Each extraction was  
 100 conducted in conical flasks for 3 h at 90 °C under continuous magnetic stirring. After extraction,  
 101 the mixture was filtered and the solid residues were washed with 100 mL distilled water. The  
 102 filtrates as well as the washed liquor were then adjusted to pH = 5.5 with 5 M HCl and  
 103 concentrated under reduced pressure.

104 **Table 1** Symbols of xylan fractions separated through different extraction and precipitation  
 105 methods.

Extraction Methods	Precipitation Methods	Xylan Fractions	Yield %*
2% NaOH	100% Ethanol	H1	9.7
4% NaOH (successive after 2%)	100% Ethanol	H2	13.0
6% NaOH (successive after 2 and 4%)	100% Ethanol	H3	7.9
2% NaOH	70% Ethanol	H4	11.5
4% NaOH	70% Ethanol	H5	17.2
6% NaOH	70% Ethanol	H6	21.6
2% NaOH	Successive precipitation with 15%, 30% and 60% ethanol	H7、 H8、 H9	3.1, 2.9, 5.6
2% NaOH	I <sub>2</sub> -KI Precipitation	H10、 H11	2.9, 6.1
2% NaOH	Ammonium sulfate	H12	7.8
Commercial xylan from sugarcane bagasse		H14	-

106 Note: \*Yield was calculated based on the oven-dried weight of the raw sugarcane bagasse.

107 The concentrated liquor was slowly poured into three volume of 100% ethanol or 70%  
108 ethanol with constant stirring. Graded ethanol precipitation (liquor successively treated by 15%,  
109 30% and 60% ethanol) (Bian et al., 2010), I<sub>2</sub>-KI precipitation (Peng et al., 2012) and ammonium  
110 sulfate precipitation (Rao and Muralikrishna, 2006) methods were also used according to  
111 previous reports. The obtained xylan samples were named as H1-H12 (Table 1). For I<sub>2</sub>-KI  
112 precipitation method, the first step was adding 0.1 volume of I<sub>2</sub>-KI solution (3 g I<sub>2</sub> and 4 g KI in  
113 100 mL water) to the concentrated liquor and the precipitated solid was denoted as solid part one  
114 (H10); the second step was taking the supernatant for dialysis (molecular weight cut off 3500)  
115 and the solid precipitated by adding three volume of 100% ethanol was denoted as solid part two  
116 (H11). The precipitated solids from each precipitation step or method were washed several times  
117 with 70% ethanol and freeze-dried. The commercial xylan (from sugarcane) purchased from  
118 Shanghai Yuanye Bio-Technology Co., Ltd (Shanghai, China) was named as H14 and used for  
119 comparison.

#### 120 *Characterization of xylan samples*

121 The xylan fractions were hydrolyzed according to previous protocols described by Min (Min  
122 et al., 2011; Min et al., 2013) and Ruiter (De Ruiter et al., 1992) in order to determine their lignin  
123 and neutral sugar, and uronic acid compositions. Neutral sugar and uronic acid concentration of  
124 the xylan hydrolysate was quantified by an Ion Chromatography system (IC-3000, Dionex, USA)  
125 equipped with an anion-exchange column (CarboPac<sup>TM</sup> PA20, Dionex, USA); the column was  
126 pre-equilibrated with 200 mM NaOH and gradiently eluted with water, 20 mM NaOH and 500  
127 mM NaAc at a flow rate of 0.5 mL/min.

128 The weight average molecular weight (M<sub>w</sub>), number average molecular weight (M<sub>n</sub>) and  
129 polydispersity index (PDI) were obtained based on the previous method by Jin (Jin et al., 2019),

130 using NaNO<sub>3</sub>-Na<sub>2</sub>HPO<sub>4</sub> solution (0.1M:0.001M) as the elution buffer. The measurement was  
131 conducted at a column temperature of 40 °C through a high performance liquid chromatography  
132 (HPLC, 1260 Infinity, Agilent Technologies, USA) equipped with GPC columns (PL  
133 aquagel-OH 60 and PL aquagel-OH MIXED-H, Agilent Technologies, USA).

134 The 2D-HSQC NMR spectra of selected xylan samples were analyzed by a 600 MHz NMR  
135 spectrometer (AVANCE III HD 600, Bruker, Germany). Approximately 20 mg of xylans was  
136 dissolved in 0.5 mL of DMSO-d<sub>6</sub>. The acquisition parameters used were 160 transients (scans  
137 per block) acquired using 1024 data points in the F2 (<sup>1</sup>H) dimension with an acquisition time of  
138 53 ms and 256 data points in the F1 (<sup>13</sup>C) dimension with an acquisition time of 5.14 ms. Total  
139 running time was 18 h. The coupling constant (<sup>1</sup>J<sub>C-H</sub>) of 147 Hz was applied.

140 The morphology of xylan aggregates in film was observed by a polarizing microscope  
141 (BX53M, Olympus, Tokyo, Japan) equipped with a U-AN360P analyzer slider. X-ray diffraction  
142 (XRD) measurements were performed in symmetric reflection mode using X'Pert Powder  
143 (Panalytical, Eindhoven, Netherlands) equipped with a copper X-ray source ( $\lambda = 1.5418 \text{ \AA}$ ) and  
144 operated at 40 kV and 40 mA. The precipitated and freeze-dried xylan samples were mounted on  
145 a powder sample holder with 200  $\mu\text{m}$ -deep central well. The sample was gently pressed and the  
146 excess above the surface level was wiped out with a flat blade. An empty holder was also  
147 measured and the intensity was subtracted from the sample data, taking the X-ray attenuation by  
148 the sample into account.

#### 149 *Preparation and Characterization of xylan films*

150 Exactly 0.51 g of xylan powder and 0.09g sorbitol as plasticizer were dispersed in 8 mL of  
151 deionized water with magnetic stirring for 30 min at 90 °C to make a 7.5 % (w/v) suspension.  
152 The suspension was poured into a Teflon mold (65 mm  $\times$  40 mm) and dried in an environmental

153 chamber regulated to a temperature of 50 °C and a relative humidity of 70 % for 24 h, allowing  
154 the formation and equilibration of xylan films. The films had a thickness of ~150 µm.

155 The film fracture surface was observed using a scanning electron microscope (SEM: Evo-18,  
156 Carl Zeiss, Germany). The tensile strength and modulus of elasticity (MOE) of the xylan films  
157 were measured using a universal tensile tester (Instron 5565, Instron, USA). At least two films  
158 were prepared from each hemicellulose fraction. Each film was cut into 4 strips (5 cm × 1 cm).  
159 The strip specimens were equilibrated and tested in a room with a constant temperature of 23 °C  
160 and a relative humidity of 50 %. Each of the 4 strip specimens was tested with a head speed of 5  
161 mm/min and a span length of 30 mm.

## 162 **Results and Discussion**

### 163 *Sugar composition*

164 The types of extraction methods of xylan used in this study are summarized in Tables 1. All  
165 separated xylyans mainly consisted of arabinose, xylose and glucuronic acid units (Table 2). As  
166 shown by the 2D-HSQC NMR spectra, arabinofuranosyl units linked to xylopyranosyl backbone  
167 through  $\alpha$ -(1-3)-linkage; glucuronopyranosyl units were 4-*O*-methylated and linked to  
168 xylopyranosyl backbone through  $\alpha$ -(1-2)-linkage (Fig. 1 and Table 3). The results are consistent  
169 with the chemical structure of glucuronoarabinoxylans extracted from graminaceous plants  
170 including sugarcane bagasse (Ebringerova and Heinze, 2000; Morais de Carvalho et al., 2017;  
171 Spiridon and Popa, 2008; Sun et al., 2000). The minor residues of galactose and galacturonic  
172 acid may come from the residual pectin component from sugarcane (de Souza et al., 2013),  
173 which was co-extracted with xylan. Some samples, e.g. H1, H4, H5, H9, H11 and H12, had high  
174 content of glucose (Table 2). 2D-HSQC spectra indicate that the glucose had its origins from

175 glucan instead of residual sucrose in the bagasse (Fig. 1 and Table 3); the existence of glucan  
 176 could be due to the alkaline degradation of cellulose (Pavasars et al., 2003). No acetylation on  
 177 the extracted xylan was observed, since alkaline treatment cleaves acetyl groups easily (Jaafar et  
 178 al., 2019). It was also found that lignin was covalently bonded to xylan (Ralph et al., 1994) by  
 179 phenyl glycoside and  $\gamma$ -ester linkages (Fig. 1 and Table 3), making a lignin-carbohydrate  
 180 complex (LCC) (Dong et al., 2020; Huang et al., 2019b); therefore, the co-extraction of lignin is  
 181 inevitable without extensive bleaching. The lignin and sugar contents do not sum up to 100%  
 182 mass balance of the xylan samples, which could be due to the undetermined ash contents and  
 183 incomplete hydrolysis or degradation to sugars during sample hydrolysis.

184 The successive alkaline treatments (H2 and H3) were able to separate xylans with high  
 185 purity excluding some inherent impurities, e.g. lignin and glucose, compared to a single alkaline  
 186 extraction (comparing between H1 and H3 in Table 2). High alkali concentration treatments (H2,  
 187 H3, H5, and H6) resulted in extraction of low degree of substitution (Table 4), corroborating  
 188 with the fact that xylan with smaller number of side groups is less soluble in water (Andrewartha  
 189 et al., 1979). Low concentration of ethanol (H7 and H8) precipitated xylans with high purity and  
 190 high molecular weight, but with low yield and low degree of substitution. By using the I<sub>2</sub>-KI  
 191 precipitation method to obtain two xylan fractions (H10 and H11), xylans was separated by  
 192 degree of substitution.

193  
 194 **Table 2** Chemical compositions of the xylan fractions separated through different extraction and  
 195 precipitation methods.

Samples	Lignin %	Arabinose %	Galactose %	Glucose %	Xylose %	Galacturonic acid %	Glucuronic acid %
Bagasse	18.2 ± 0.3	1.4 ± 0.1	0.4 ± 0.0	33.9 ± 1.7	21.6 ± 1.3	1.4 ± 0.1	3.7 ± 0.2
H1	3.6 ± 1.7	8.0 ± 0.8	1.8 ± 0.1	11.4 ± 2.4	53.0 ± 0.6	2.2 ± 0.2	3.8 ± 0.2
H2	2.9 ± 0.0	6.5 ± 0.1	0.4 ± 0.1	3.5 ± 0.3	65.4 ± 0.7	1.4 ± 0.0	2.9 ± 0.3

H3	2.7 ± 0.3	5.7 ± 0.3	0.3 ± 0.0	3.1 ± 0.1	76.2 ± 0.9	1.3 ± 0.0	2.6 ± 0.1
H4	6.1 ± 1.0	7.1 ± 0.2	0.9 ± 0.0	9.0 ± 1.1	57.6 ± 0.3	2.3 ± 0.0	4.4 ± 0.3
H5	4.7 ± 1.6	5.2 ± 0.0	0.6 ± 0.0	7.3 ± 0.8	58.5 ± 1.3	1.8 ± 0.1	3.1 ± 0.2
H6	5.1 ± 1.0	5.3 ± 0.2	0.6 ± 0.0	3.3 ± 0.0	57.6 ± 0.3	1.5 ± 0.0	3.4 ± 0.2
H7	11.4 ± 0.4	6.0 ± 0.8	0.5 ± 0.0	3.8 ± 0.2	70.7 ± 1.1	1.8 ± 0.0	2.3 ± 0.3
H8	4.7 ± 0.0	7.3 ± 0.1	0.4 ± 0.0	4.8 ± 0.0	66.2 ± 0.2	2.4 ± 0.1	4.1 ± 0.1
H9	8.3 ± 0.9	8.4 ± 0.3	1.8 ± 0.3	9.9 ± 0.5	50.1 ± 0.1	1.4 ± 0.1	4.7 ± 1.2
H10	16.3 ± 0.9	4.3 ± 0.3	0.3 ± 0.1	3.4 ± 0.9	50.2 ± 0.7	1.3 ± 0.0	2.7 ± 0.0
H11	10.2 ± 1.3	8.5 ± 0.2	1.8 ± 0.0	18.0 ± 0.5	50.6 ± 1.4	2.3 ± 0.0	2.8 ± 0.0
H12	4.2 ± 0.1	7.0 ± 0.1	0.6 ± 0.1	7.8 ± 0.1	61.8 ± 0.2	2.0 ± 0.0	2.3 ± 0.2
H14	1.6 ± 0.3	7.5 ± 0.2	1.7 ± 0.0	1.4 ± 0.1	76.5 ± 1.9	1.3 ± 0.0	3.9 ± 0.1

196

197

198 **Table 3** Peak assignments of the HSQC spectra of xylans associated with Fig. 1.

Labels	$\delta_C/\delta_H$	Assignment
Lignin structure		
-OCH <sub>3</sub>	55.9/3.73	C-H in methoxyls
A <sub>γ</sub>	59.6-60.8/3.37-3.72	C <sub>γ</sub> -H <sub>γ</sub> in β-O-4 substructures(A)
A <sub>γ'</sub>	63.6/3.86	C <sub>γ</sub> -H <sub>γ</sub> in γ-acylated β-O-4 substructures (A')
A <sub>β(S)</sub>	86.0/3.91	C <sub>β</sub> -H <sub>β</sub> in β-O-4 substructures linked to a S unit (A)
A <sub>α</sub>	72.8/4.86	C <sub>α</sub> -H <sub>α</sub> in phenylcoumaran substructures (C)
Associated carbohydrate and LCCs linkages		
X <sub>1+Glu1</sub>	103.2/4.21	C <sub>1</sub> -H <sub>1</sub> in β-(1→4)-D-xylopyranoside C <sub>1</sub> -H <sub>1</sub> in β-(1→4)-D-Glucan
X <sub>2</sub>	72.5/3.02	C <sub>2</sub> -H <sub>2</sub> in β-(1→4)-D-xylopyranoside
X <sub>3</sub>	73.5/3.25	C <sub>3</sub> -H <sub>3</sub> in β-(1→4)-D-xylopyranoside
X <sub>4</sub>	75.4/3.50	C <sub>4</sub> -H <sub>4</sub> in β-(1→4)-D-xylopyranoside
X <sub>5</sub>	62.6/3.20	C <sub>5</sub> -H <sub>5</sub> in β-(1→4)-D-xylopyranoside
X <sub>NR4</sub>	69.5/3.24	C <sub>4</sub> -H <sub>4</sub> in β-(1→4)-D-xylopyranoside with non-reducing end
X <sub>NR5</sub>	65.5/3.01,3.45	C <sub>5</sub> -H <sub>5</sub> in β-(1→4)-D-xylopyranoside with non-reducing end
X2 <sub>1</sub>	99.4/4.42	C <sub>1</sub> -H <sub>1</sub> in β-(1→4)-D-Xylp-2-O-(4-O-methyl-α-D-GlcUA)
Ara <sub>1</sub>	106.9/5.32	C <sub>1</sub> -H <sub>1</sub> in α-(1→3)-L-arabinofuranoside
Ara <sub>2</sub>	81.6/3.79	C <sub>2</sub> -H <sub>2</sub> in α-(1→3)-L-arabinofuranoside

Ara <sub>3</sub>	77.1/3.62	C <sub>3</sub> -H <sub>3</sub> in $\alpha$ -(1→3)-L-arabinofuranoside
Ara <sub>4</sub>	85.9/3.89	C <sub>4</sub> -H <sub>4</sub> in $\alpha$ -(1→3)-L-arabinofuranoside
Ara <sub>5</sub>	61.9/3.52	C <sub>5</sub> -H <sub>5</sub> in $\alpha$ -(1→3)-L-arabinofuranoside
U <sub>1</sub>	97.2/4.98	C <sub>1</sub> -H <sub>1</sub> in 4- <i>O</i> -methyl- $\alpha$ -D-GlcUA
U <sub>4</sub>	81.9/3.08	C <sub>4</sub> -H <sub>4</sub> in 4- <i>O</i> -methyl- $\alpha$ -D-GlcUA
U <sub>5</sub>	72.9/4.28	C <sub>5</sub> -H <sub>5</sub> in 4- <i>O</i> -methyl- $\alpha$ -D-GlcUA
Glu <sub>4</sub>	73.8/3.62	C <sub>4</sub> -H <sub>4</sub> in $\beta$ -(1→4)-D-Glucan
Glu <sub>5</sub>	73.4/3.45	C <sub>5</sub> -H <sub>5</sub> in $\beta$ -(1→4)-D-Glucan
Est+A <sub><math>\gamma</math></sub>	65-62/3.5-4.0	$\gamma$ -ester and A' $\gamma$ in LCC
PhGlc2	100.9/4.63	Phenyl glycoside-2 in LCC

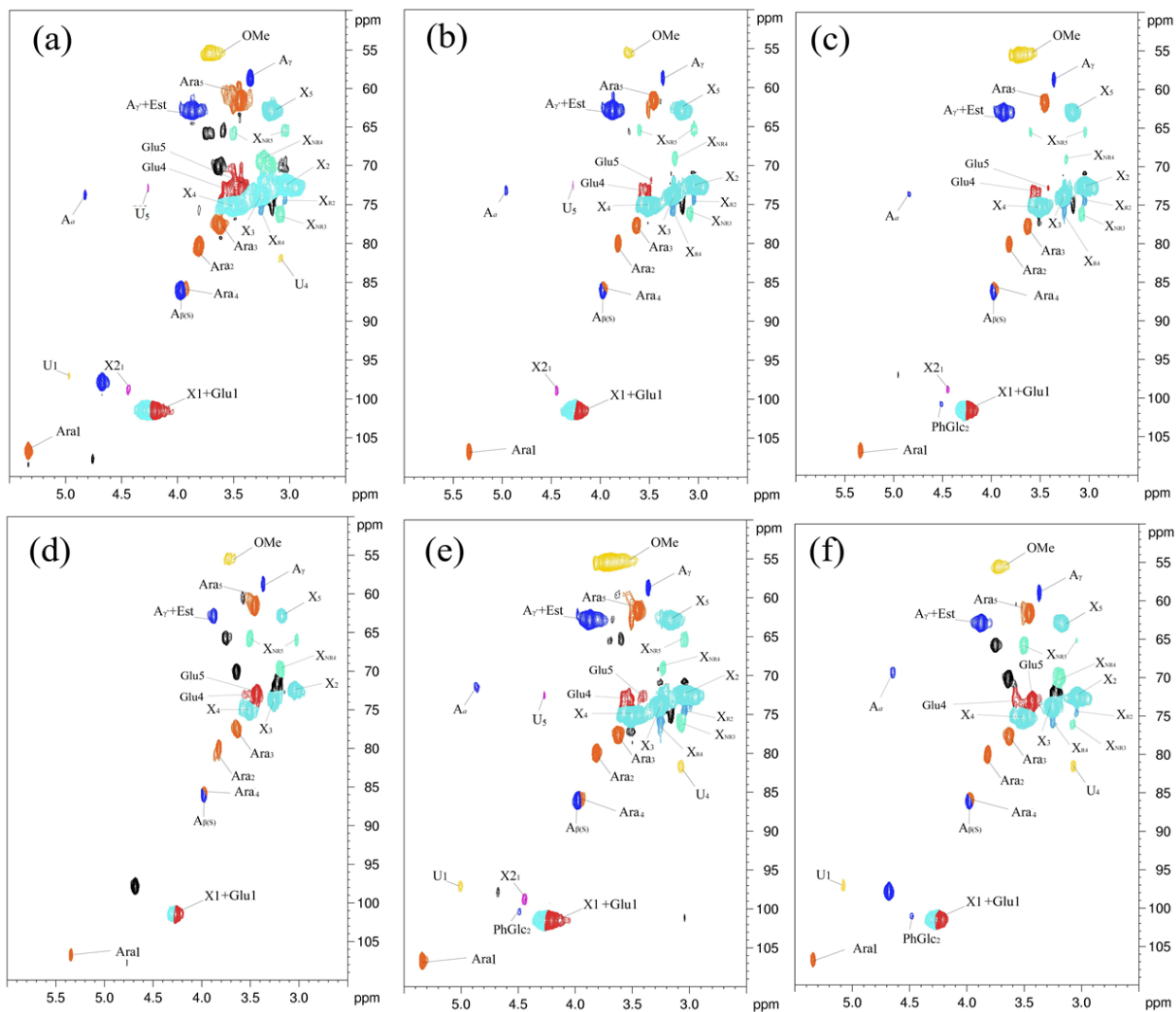
199

200

201 **Table 4** Molecular structures and film forming ability for the separated xylan fractions.

Xylan Fractions	Mn	Mw	PI	Degree of substitution*	Film Formable
H1	33500	61300	1.83	0.224 ± 0.016	Yes
H2	29700	61500	2.07	0.143 ± 0.005	No
H3	25100	66400	2.64	0.109 ± 0.004	No
H4	40200	63700	1.58	0.200 ± 0.004	Yes
H5	29800	52000	1.74	0.142 ± 0.007	No
H6	27500	52300	1.90	0.151 ± 0.000	No
H7	41300	67600	1.64	0.124 ± 0.003	No
H8	45500	71900	1.58	0.172 ± 0.003	Yes
H9	13800	60500	4.39	0.261 ± 0.017	Yes
H10	40300	64400	1.60	0.139 ± 0.008	No
H11	34200	61000	1.78	0.223 ± 0.002	Yes
H12	39500	61600	1.56	0.150 ± 0.001	Yes
H14	17500	58000	3.31	0.149 ± 0.002	No

202 Note: \*Degree of substitution was calculated by the content ratio of (arabinose+ glucuronic acid)/xylose.



203  
 204 **Figure 1** HSQC spectra of xylan fractions H1 (a), H3 (b), H7 (c), H9 (d), H10 (e), H11(f).

205  
 206  
 207 **Film formation**  
 208 When cast in a Teflon mold from aqueous solution/suspension, samples H1, H4, H8, H9,  
 209 H11, H12 were able to form integral films without apparent cracks; we call these samples “film  
 210 forming” (Fig. 2 & Table 4). Samples H5, H7, H10 formed films but with long cracks and  
 211 samples H2, H3, H6, H14 broke into small fragments; we qualify both as not film forming.

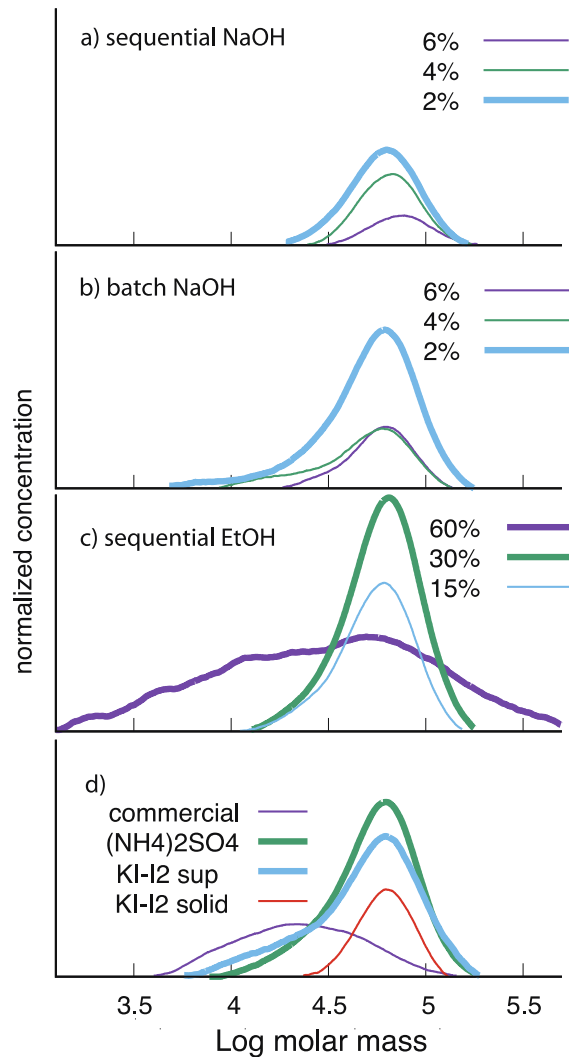


**Figure 2** The films casted in Teflon molds.

212  
213  
214  
215  
216  
217  
218  
219  
220  
221  
222  
223  
224  
225  
226  
227  
228  
229

The xylans able to form films generally had high degree of substitution. A critical value of degree of substitution of about 0.15 can be identified above which an integral film is formed in our casting condition. Samples H6, H12 and H14 had degree of substitution values of 0.15, but only H12 formed a film. H12 had higher glucose content (Table 2), which corroborates the need for the addition of external plasticizers or biopolymers is helpful to the film formation of xylan (Gabrielii and Gatenholm, 1998; Grondahl et al., 2004; Kayserilioglu et al., 2003). The lignin contents in film-forming fraction were in the range of 1.6-16 %, while those in the other fractions were in range of 3.6-10 %, indicating lignin is not influencing xylan film formation. This contradicts the finding of the previous study that low content of lignin is necessary to xylan film formation (Goksu et al., 2007), and the previous result might have been a pure coincidence.

We do not know whether different side groups, i.e. arabinose and glucuronic acid, have specific influences on the film formability of xylans. The alkaline extracted xylans in this study were deacetylated, so the effect of acetyl groups on the film formability was not determined.



230

231 **Figure 3** The molecular weight distributions of xylan samples extracted by different methods.  
 232 The elution profile was normalized with the quantity injected, so the area is proportional to the  
 233 soluble fraction in the elution buffer (0.1M NaNO<sub>3</sub>-Na<sub>2</sub>HPO<sub>4</sub> at 40°C).

234

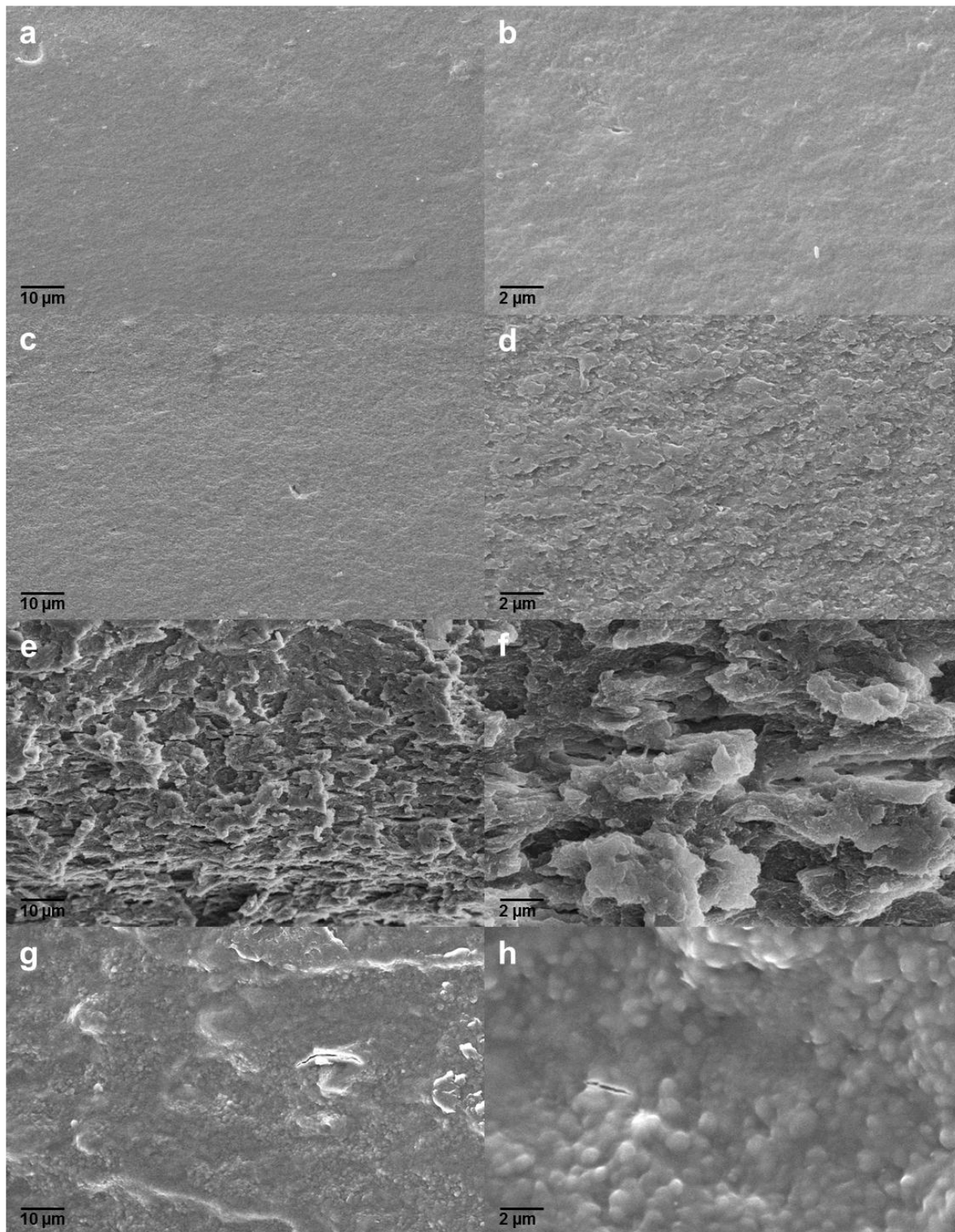
235 The molecular weight distribution calibrated with dextran standard is shown in Figure 3. All  
 236 samples except H9 (last fraction of sequential precipitation with increasing concentration of  
 237 ethanol) and commercial xylan (H14) showed similar distribution. The elution profile was  
 238 normalized with the quantity injected, so the area is proportional to the soluble fraction in the  
 239 elution buffer (0.1M NaNO<sub>3</sub>-Na<sub>2</sub>HPO<sub>4</sub> at 40°C). The film forming samples are shown in thick  
 240 lines in Figure 3. In each series, only the samples having high soluble fraction were forming films.

241 ***Film microstructure***

242 The SEM images showed that the film fracture surface (at the natural cracking position for  
243 broken films) was smooth for film forming samples (Fig. 4 a&b). On the other hand, films that  
244 were cracked during drying showed flake-like granular morphology (Fig. 4 c-f) or spherical  
245 shape (Fig. 4 g&h) for the sample fragmented in small pieces. When observed under crossed  
246 polarizers, the films showed little birefringence (Fig. 5 a-c), while the broken films showed a  
247 large number of birefringent granular objects (Fig. 5 d-f).

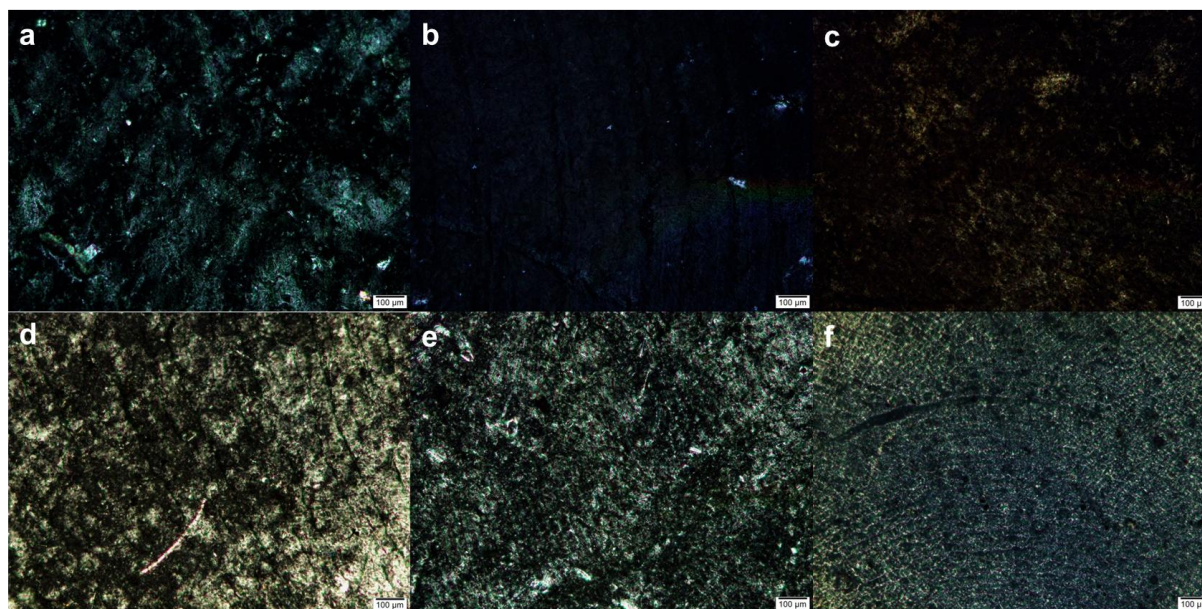
248 The suspensions of xylan samples that showed fragmentation during cast-drying showed  
249 low viscosity and milky appearance (Fig. S1a and Table S1), in which some suspensions would  
250 settle after standing, indicating large xylan particles are already present in the suspension, and  
251 free chains are not abundant. The suspensions of xylan samples that form integral films showed  
252 high viscosity and gel-like property with some transparency (Fig. S1b and Table S1), indicating  
253 limited formation of xylan particles and presence of more free chains. The aggregates present  
254 already in the suspension probably limit the film formability.

255



256

257 **Figure 4** SEM images of the film cross-section (from the natural cracking position for broken  
 258 films) for (a)(b) H4-F, (c)(d) H5-NF, (e)(f) H7-NF, and (g)(h) H14-NF. Note: “F” means sample  
 259 formed an integral film; “NF” means sample formed broken films.



260

261 **Figure 5** Cross-polarized microscopic images of xylan films (a) H1-F, (b) H8-F, (c) H11-F, (d)  
 262 H5-NF, (e) H7-NF, and (f) H14-NF. Scale bar = 100 μm. Note: “F” means sample formed an  
 263 integral film; “NF” means sample formed broken films.

264

265 ***Crystallinity***

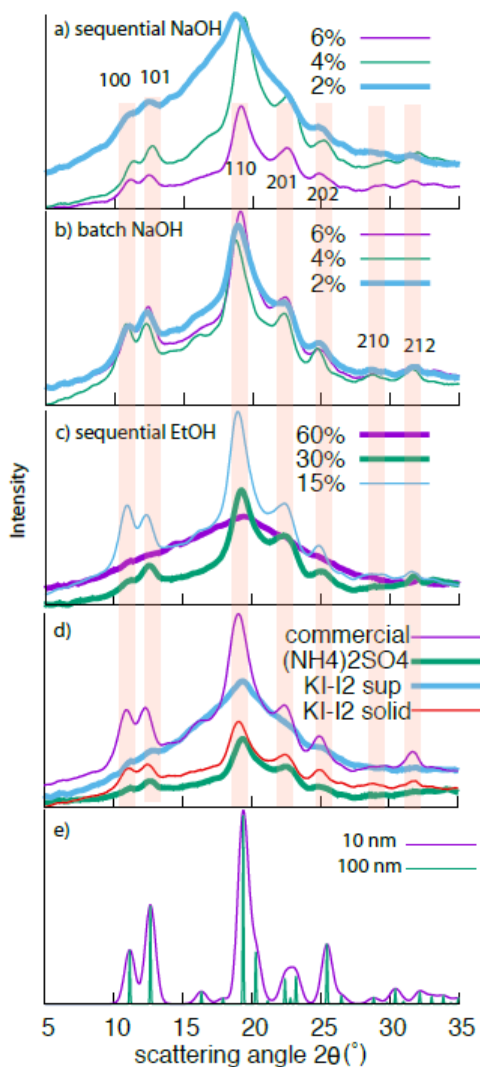
266 Xylan is generally considered as an amorphous polymer, but the unsubstituted segment of  
 267 xylan form hydrous and anhydrous crystals (Dea et al., 1973; Hoije et al., 2008; Horio and  
 268 Imamura, 1964; Kobayashi et al., 2013; Marchessault and Timell, 1960; Nieduszynski and  
 269 Marchessault, 1972). Indeed, in a sequential extraction the first extraction is quite amorphous  
 270 while a successive extraction is more crystalline (Fig. 6a). In the single extraction, the fraction  
 271 that can be extracted by 2% NaOH is less crystalline (Fig. 6b). The precipitation in the single  
 272 extraction was done with 70% ethanol, so the 2% NaOH in this extraction was slightly more  
 273 crystalline than in the sequential series. When xylan was sequentially precipitated with different  
 274 ethanol concentration, from lower to higher, the first precipitates are crystalline while the last  
 275 precipitate that can only be precipitated at high ethanol concentration is amorphous (Fig. 6c).  
 276 Finally the direct precipitate with KI-I<sub>2</sub> was crystalline while the supernatant was amorphous. In

277 general the amorphous samples were film forming (thick lines in Fig. 6) whereas highly  
278 crystalline samples were cracked during drying. In addition, as each sample had slightly different  
279 peak positions indicating that the crystal structures are not exactly the same among samples, we  
280 did not calculate crystallinity index or crystallite sizes of xylan that would not be reliable.  
281 However, the general aspect of XRD profiles is sufficiently different among samples to allow for  
282 qualitative comparison.

283 The calculated diffraction profile based on the atomic coordinate proposed by Nieduszynski  
284 and Marchessault (1972) is given in Figure 6e (cif file of the structure is given in supplementary  
285 material). The general diffraction features agree roughly with the model, and the miller indices of  
286 peaks of the reflections mainly contributing to the peaks, as judged from the reported fiber  
287 diffraction diagram and calculated intensities are indicated in the Figure 6. This xylan in this  
288 structure form three-fold helix in contrast to the two-fold helix of cellulose or xylan adsorbed on  
289 cellulose surface (Falcoz-Vigne et al., 2017; Ling et al., 2020; Martínez-Abad et al., 2017).

290 The presence of side groups seems to play role in preventing the crystallization/excessive  
291 aggregation of xylan molecules (Andrewartha et al., 1979; Dea et al., 1973; Hoije et al., 2008;  
292 Shrestha et al., 2019) (Table 4 and Figs. 4-6); for example, samples H1 and H9 had high degree  
293 of substitution and showed almost amorphous XRD diffraction patterns. We did not find  
294 evidence of different side groups, i.e. arabinose and glucuronic acid, having different influences  
295 on the crystallization of xylans. The carbohydrate impurities, e.g. galactose, glucose and  
296 galacturonic acid (Table 2), were also found to be related to the low crystallinity of xylans, e.g.  
297 sample H11; this is similar to other biopolymers, e.g. starch, for which artificial additives are  
298 also able to prevent the aggregation (Fama et al., 2005). The lignin content was not found to be  
299 very relevant to the xylan crystallization (Table 2). Its hydrophobic nature results in the

300 incompatibility to the hydrophilic xylan (Baumberger et al., 1998), and as a consequence, would  
 301 be less effective in preventing the xylan from aggregation. The excessive aggregation of xylan  
 302 molecules affects the solubility and solution/suspension viscosity (Andrewartha et al., 1979; Dea  
 303 et al., 1973; Nieduszynski and Marchessault, 1972; Shrestha et al., 2019). Our results suggest  
 304 that the prevention of excessive aggregation of xylan molecules, which is assisted by the xylan  
 305 side chains or impurities, is highly related to the film forming capacity of xylans.



306  
 307 **Figure 6** a-d) X-ray diffraction profiles of freeze-dried xylans after subtraction of air scattering  
 308 and sample holder (thick lines indicate the film forming samples). The Miller indices of major  
 309 peaks based on trigonal unit cell in the study of (Nieduszynski and Marchessault, 1972) are  
 310 indicated. e) Simulated powder diffraction based on Nieduszynski's monohydrate structure with  
 311 isotropic crystallite size of 10 nm (violet) or 100 nm (green).

312 ***Film mechanical properties***

313 The six integral film samples were tested for their mechanical properties including tensile  
314 strength and modulus of elasticity (MOE). Samples H1, H4, and H11 had the highest tensile  
315 strength of 12~14 MPa and MOE of 150~180 MPa, while H8, H9, and H12 had much lower  
316 values (Table 5). Once the xylan is able to form a film, the film mechanical property is no longer  
317 positively related to the degree of substitution or negatively correlated to crystallinity. Samples  
318 H1, H4 and H11 had a medium degree of substitution, but had the highest mechanical properties,  
319 i.e. tensile strength and MOE; sample H9 had the highest degree of substitution of 0.261 and  
320 showed an almost amorphous XRD diffraction pattern, but had low mechanical properties. This  
321 is consistent with previous studies that moderate degree of substitution improved, while high  
322 degree of substitution was detrimental to the xylan film tensile strength (Hoiije et al., 2008; Jin et  
323 al., 2019). It can be concluded that the regulating mechanisms to xylan film formation and xylan  
324 film mechanical properties are different. The side groups of xylan molecules prevent their  
325 aggregation or crystallization, facilitating the film formation, but once the film is formed, the  
326 side groups do not seem to be necessarily contributing to the mechanical resistance.

327

328 **Table 5** Xylan film mechanical properties ( $\pm$  standard error).

Xylan Samples		Tensile Strength (MPa)	MOE (MPa)
H1	High	$13.7 \pm 1.8$	$182 \pm 19$
H4		$13.2 \pm 2.2$	$150 \pm 15$
H11		$11.6 \pm 1.7$	$171 \pm 42$
H9	Low	$4.8 \pm 0.4$	$99 \pm 13$
H12		$4.5 \pm 0.3$	$38 \pm 5$
H8		$1.4 \pm 0.1$	$14 \pm 2$

329

## 330 **Conclusion**

331 Bagasse xylan could be fractionated as function of side group densities using either severity  
332 of extracting conditions or precipitation conditions, with the higher density side groups being  
333 easier to extract and difficult to precipitate, with relatively constant molecular weight distribution  
334 as measured by gel permeation chromatography. The side group density was directly correlated  
335 with the crystallinity of freeze-dried samples. The excessive aggregation or crystallization of  
336 xylan, which can be effectively prevented by the side chains of xylans or impurities, **i.e. lignin**  
337 **and glucan**, is detrimental to the water-cast film forming ability of xylans. However, once a  
338 xylan film is formed, the crystallinity contributes to the higher stiffness and strength of the film.  
339 This finding would contribute to rational fractionation and xylan modification for material  
340 processing with controlled properties. **We focused on alkaline extraction in this study, but will**  
341 **further evaluate milder extraction conditions such as hot-water extraction at neutral pH or**  
342 **DMSO extraction that can keep acetyl groups which might also contribute to the film**  
343 **formability.**

## 344 **Acknowledgements**

345 This work was supported by the National Natural Science Foundation of China (31600470),  
346 Guangzhou Science and Technology Program (General Scientific Research Project  
347 201707010053), and Guangdong Province Science Foundation for Cultivating National  
348 Engineering Research Center for Efficient Utilization of Plant Fibers (2017B090903003). The  
349 authors greatly thank the anonymous reviewer for the detailed analysis of the reported crystal  
350 structure of xylans.

351 **References**

- 352 Andrewartha KA, Phillips DR, Stone BA (1979) Solution properties of wheat-flour arabinoxylans and  
353 enzymically modified arabinoxylans. *Carbohyd Res* 77:191-204.
- 354 Arinstein A, Burman M, Gendelman O, Zussman E (2007) Effect of supramolecular structure on polymer  
355 nanofibre elasticity. *Nat Nanotechnol* 2:59-62.
- 356 Baumberger S, Lapierre C, Monties B, Della Valle G (1998) Use of kraft lignin as filler for starch films.  
357 *Polym Degrad Stabil* 59:273-277.
- 358 Bian J, Peng F, Peng P, Xu F, Sun RC (2010) Isolation and fractionation of hemicelluloses by graded  
359 ethanol precipitation from *Caragana korshinskii*. *Carbohyd Res* 345:802-809.
- 360 De Rosa C, Auriemma F, de Ballesteros OR (2006) The role of crystals in the elasticity of semicrystalline  
361 thermoplastic elastomers. *Chem Mater* 18:3523-3530.
- 362 De Ruiter GA, Schols HA, Voragen AGJ, Rombouts FM (1992) Carbohydrate analysis of water-soluble  
363 uronic acid-containing polysaccharides with high-performance anion-exchange chromatography using  
364 methanolysis combined with TFA hydrolysis is superior to four other methods. *Analytical Biochemistry*  
365 207:176-185.
- 366 de Souza AP, Leite DCC, Pattathil S, Hahn MG, Buckeridge MS (2013) Composition and Structure of  
367 Sugarcane Cell Wall Polysaccharides: Implications for Second-Generation Bioethanol Production.  
368 *BioEnergy Research* 6:564-579.
- 369 Dea ICM, Rees DA, Beveridge RJ, Richards GN (1973) Aggregation with change of conformation in  
370 solutions of hemicellulose xylans. *Carbohyd Res* 29:363-372.
- 371 Dong H, Zheng L, Yu P, Jiang Q, Wu Y, Huang C, Yin B (2020) Characterization and Application of  
372 Lignin–Carbohydrate Complexes from Lignocellulosic Materials as Antioxidants for Scavenging In Vitro  
373 and In Vivo Reactive Oxygen Species. *Acs Sustain Chem Eng* 8:256-266.
- 374 Ebringerova A, Heinze T (2000) Xylan and xylan derivatives - biopolymers with valuable properties, 1 -  
375 Naturally occurring xylans structures, procedures and properties. *Macromol Rapid Comm* 21:542-556.
- 376 Falcoz-Vigne L, Ogawa Y, Molina-Boisseau S, Nishiyama Y, Meyer V, Petit-Conil M, Mazeau K, Heux L  
377 (2017) Quantification of a tightly adsorbed monolayer of xylan on cellulose surface. *Cellulose*  
378 24:3725-3739.
- 379 Fama L, Rojas AM, Goyanes S, Gerschenson L (2005) Mechanical properties of tapioca-starch edible films  
380 containing sorbates. *Lwt-Food Sci Technol* 38:631-639.
- 381 Gabriellii I, Gatenholm P (1998) Preparation and properties of hydrogels based on hemicellulose. *J Appl*  
382 *Polym Sci* 69:1661-1667.
- 383 Goksu EI, Karamanlioglu M, Bakir U, Yilmaz L, Yilmazer U (2007) Production and characterization of films  
384 from cotton stalk xylan. *J Agr Food Chem* 55:10685-10691.
- 385 Grondahl M, Eriksson L, Gatenholm P (2004) Material properties of plasticized hardwood Xylans for  
386 potential application as oxygen barrier films. *Biomacromolecules* 5:1528-1535.
- 387 Hansen NML, Plackett D (2008) Sustainable films and coatings from hemicelluloses: A review.  
388 *Biomacromolecules* 9:1493-1505.
- 389 Hoije A, Grondahl M, Tommeraas K, Gatenholm P (2005) Isolation and characterization of  
390 physicochemical and material properties of arabinoxylans from barley husks. *Carbohyd Polym*  
391 61:266-275.
- 392 Hoije A, Sternemalm E, Heikkinen S, Tenkanen M, Gatenholm P (2008) Material properties of films from  
393 enzymatically tailored arabinoxylans. *Biomacromolecules* 9:2042-2047.
- 394 Horio M, Imamura R (1964) Crystallographic study of xylan from wood. *Journal of Polymer Science Part A:*  
395 *General Papers* 2:627-644.

396 Huang C, Lin W, Lai C, Li X, Jin Y, Yong Q (2019a) Coupling the post-extraction process to remove residual  
397 lignin and alter the recalcitrant structures for improving the enzymatic digestibility of acid-pretreated  
398 bamboo residues. *Bioresource Technol* 285:121355.

399 Huang C, Wang X, Liang C, Jiang X, Yang G, Xu J, Yong Q (2019b) A sustainable process for procuring  
400 biologically active fractions of high-purity xylooligosaccharides and water-soluble lignin from Moso  
401 bamboo prehydrolyzate. *Biotechnology for biofuels* 12:189.

402 Jaafar Z, Mazeau K, Boissière A, Le Gall S, Villares A, Vigouroux J, Beury N, Moreau C, Lahaye M, Cathala  
403 B (2019) Meaning of xylan acetylation on xylan-cellulose interactions: A quartz crystal microbalance with  
404 dissipation (QCM-D) and molecular dynamic study. *Carbohyd Polym* 226:115315.

405 Jin XC, Hu ZH, Wu SF, Song T, Yue FX, Xiang ZY (2019) Promoting the material properties of xylan-type  
406 hemicelluloses from the extraction step. *Carbohyd Polym* 215:235-245.

407 Kayserilioglu BS, Bakir U, Yilmaz L, Akkas N (2003) Use of xylan, an agricultural by-product, in wheat  
408 gluten based biodegradable films: mechanical, solubility and water vapor transfer rate properties.  
409 *Bioresource Technol* 87:239-246.

410 Kobayashi K, Kimura S, Heux L, Wada M (2013) Crystal transition between hydrate and anhydrous (1 ->  
411 3)-beta-D-xylan from *Penicillium dumetosus*. *Carbohyd Polym* 97:105-110.

412 Lin W, Chen D, Yong Q, Huang C, Huang S (2019) Improving enzymatic hydrolysis of acid-pretreated  
413 bamboo residues using amphiphilic surfactant derived from dehydroabiatic acid. *Bioresource Technol*  
414 293:122055.

415 Ling Z, Edwards JV, Nam S, Xu F, French AD (2020) Conformational analysis of xylobiose by DFT quantum  
416 mechanics. *Cellulose* 27:1207-1224.

417 Marchessault RH, Timell TE (1960) THE X-RAY PATTERN OF CRYSTALLINE XYLANS. *The Journal of Physical*  
418 *Chemistry* 64:704-704.

419 Martínez-Abad A, Berglund J, Toriz G, Gatenholm P, Henriksson G, Lindström M, Wohler J, Vilaplana F  
420 (2017) Regular Motifs in Xylan Modulate Molecular Flexibility and Interactions with Cellulose Surfaces.  
421 *Plant Physiology* 175:1579.

422 Mikkonen KS, Heikkinen S, Soovre A, Peura M, Serimaa R, Talja RA, Helén H, Hyvönen L, Tenkanen M  
423 (2009) Films from oat spelt arabinoxylan plasticized with glycerol and sorbitol. *J Appl Polym Sci*  
424 114:457-466.

425 Min DY, Li QZ, Jameel H, Chiang V, Chang HM (2011) Comparison of pretreatment protocols for  
426 cellulase-mediated saccharification of wood derived from transgenic low-xylan lines of cottonwood (*P.*  
427 *trichocarpa*). *Biomass Bioenerg* 35:3514-3521.

428 Min DY, Yang CM, Shi R, Jameel H, Chiang V, Chang HM (2013) The elucidation of the lignin structure  
429 effect on the cellulase-mediated saccharification by genetic engineering poplars (*Populus nigra* L. x  
430 *Populus maximowiczii* A.). *Biomass Bioenerg* 58:52-57.

431 Morais de Carvalho D, Martínez-Abad A, Evtuguin DV, Colodette JL, Lindström ME, Vilaplana F,  
432 Sevastyanova O (2017) Isolation and characterization of acetylated glucuronoarabinoxylan from  
433 sugarcane bagasse and straw. *Carbohyd Polym* 156:223-234.

434 Nieduszynski IA, Marchessault RH (1972) Structure of  $\beta$ ,D(1 $\rightarrow$ 4')-xylan hydrate. *Biopolymers*  
435 11:1335-1344.

436 Pavasars I, Hagberg J, Borén H, Allard B (2003) Alkaline Degradation of Cellulose: Mechanisms and  
437 Kinetics. *J Polym Environ* 11:39-47.

438 Peng F, Bian J, Ren JL, Peng P, Xu F, Sun RC (2012) Fractionation and characterization of alkali-extracted  
439 hemicelluloses from peashrub. *Biomass Bioenerg* 39:20-30.

440 Ralph J, Hatfield RD, Quideau S, Helm RF, Grabber JH, Jung H-JG (1994) Pathway of p-Coumaric Acid  
441 Incorporation into Maize Lignin As Revealed by NMR. *J Am Chem Soc* 116:9448-9456.

442 Rao MVSSTS, Muralikrishna G (2006) Hemicelluloses of ragi (finger millet, *Eleusine coracana*, indaf-15):  
443 Isolation and purification of an alkali-extractable arabinoxylan from native and malted hemicellulose B. J  
444 Agr Food Chem 54:2342-2349.

445 Shrestha UR, Smith S, Pingali SV, Yang H, Zahran M, Breunig L, Wilson LA, Kowali M, Kubicki JD, Cosgrove  
446 DJ, O'Neill HM, Petridis L (2019) Arabinose substitution effect on xylan rigidity and self-aggregation.  
447 Cellulose 26:2267-2278.

448 Spiridon I, Popa VI (2008) Chapter 13 - Hemicelluloses: Major Sources, Properties and Applications. In:  
449 Belgacem MN, Gandini A (eds). Monomers, Polymers and Composites from Renewable Resources.  
450 Elsevier, Amsterdam. pp 289-304

451 Sternemalm E, Hoije A, Gatenholm P (2008) Effect of arabinose substitution on the material properties  
452 of arabinoxylan films. Carbohyd Res 343:753-757.

453 Sun RC, Tomkinson J, Ma PL, Liang SF (2000) Comparative study of hemicelluloses from rice straw by  
454 alkali and hydrogen peroxide treatments. Carbohyd Polym 42:111-122.

455 Xiang ZY, Watson J, Tobimatsu Y, Runge T (2014) Film-forming polymers from distillers' grains: structural  
456 and material properties. Ind Crop Prod 59:282-289.

457